JOURNAL OF BACTERIOLOGY, July 1992, p. 4416–4426
0021-9193/92/134416-11$02.00/0

Vol. 174, No. 13

Rhizobium meliloti Mutants Unable To Synthesize Anthranilate Display a Novel Symbiotic Phenotype

GARY D. BARSOMIAN,† ANA URZAINQUI,‡ KARIN LOHMAN,§ AND GRAHAM C. WALKER*

Department of Biology, Massachusetts Institute of Technology, 77 Massachusetts Avenue, Cambridge, Massachusetts 02139

Received 19 August 1991/Accepted 27 April 1992

Analyses of *Rhizobium meliloti trp* auxotrophs suggest that anthranilate biosynthesis by the *R. meliloti trpE(G)* gene product is necessary during nodule development for establishment of an effective symbiosis. *trpE(G)* mutants, as well as mutants blocked earlier along this pathway in aromatic amino acid biosynthesis, form nodules on alfalfa that have novel defects. In contrast, *R. meliloti trp* mutants blocked later in the tryptophan-biosynthetic pathway form normal, pink, nitrogen-fixing nodules. *trpE(G)* mutants form two types of elongated, defective nodules containing unusually extended invasion zones on alfalfa. One type contains bacteroids in its base and is capable of nitrogen fixation, while the other lacks bacteroids and cannot fix nitrogen. The *trpE(G)* gene is expressed in normal nodules. Models are discussed to account for these observations, including one in which anthranilate is postulated to act as an in planta siderophore.

Bacteria of the genus *Rhizobium* can fix nitrogen in symbiosis with leguminous plants. Differentiated bacteria, called bacteroids, fix nitrogen within specialized structures termed root nodules. Establishment of this symbiosis requires a complex series of developmental changes involving differentiation of both plant and bacterial cells (14, 17, 21, 22). In an early stage of this process, bacteria trapped in a curled root hair, or shepherd's crook, induce the formation of an invasion tube called an infection thread. At the same time, root cortical cells start dividing to begin nodule formation. The infection thread containing the invading microbes extends down the root hair into the developing nodule, where it branches and delivers bacteria into many plant cells. These released intracellular bacteria are surrounded by a plant membrane named the peribacteroid membrane. They then differentiate into nitrogen-fixing forms termed bacteroids and synthesize the various proteins required for nitrogen fixation.

The *Rhizobium meliloti-Medicago sativa* symbiosis is an extensively studied example of this complex plant-bacterium interaction. Many of the bacterial genes involved in symbiosis have been identified by mutations which cause a defect in symbiosis and perturbation of symbiotic development. For example, strains which are mutant in certain *nod* genes do not induce formation of nodules or nodulelike structures and are apparently blocked at the earliest stage of symbiotic development (6). These mutants do not curl root hairs, nor do they induce cortical cell divisions. Strains mutant in production of the periplasmic cyclic glucan (*ndv* mutants) or the acidic exopolysaccharide (*exo* mutants) form small white nodules devoid of bacteria, indicating that these genes are required for nodule invasion (16, 17). Finally, strains mutant in any of the *nif* or *fix* genes induce nodules which are morphologically mature but which fail to fix nitrogen. These genes are involved in the metabolism necessary for nitrogen fixation in mature nodules (5, 13).

In this study, we analyzed the symbiotic phenotypes of *R. meliloti trp* mutants. The tryptophan biosynthetic pathway has been examined in detail in many prokaryotic systems and is essentially the same in each (4), except for the arrangement and regulation of the genes involved. By analyzing the ability of R′ plasmids carrying *R. meliloti* DNA to complement *R. leguminosarum* and *Pseudomonas aeruginosa trp* mutants, Johnston and Beringer (15) were able to show that the *R. meliloti trp* genes are present in three unlinked chromosomal groups, containing *trpE*, *trpC*, and *trpD*, and *trpA*, *trpB*, and *trpF*, respectively. The *R. meliloti trpE* locus, identified by heterologous complementation, has subsequently been shown by Bae et al. (1) to be a fusion between the *trpE* and *trpG* coding sequences and has been named *trpE(G)*.

In this report, we describe the isolation and characterization of a set of tryptophan auxotrophs of *R. meliloti*. Of particular interest were *R. meliloti trpE(G)* mutants, since we show that these mutants, blocked at the first step in tryptophan biosynthesis, are ineffective symbionts, while mutants blocked at later steps are symbiotically effective.

MATERIALS AND METHODS

Strains, plasmids, and media. The bacterial strains and plasmids used are listed in Table 1. Bacteria were grown in LB medium (19) with 2.5 mM $MgSO_4$ and 2.5 mM $CaCl_2$ added for *R. meliloti* cultures. The minimal medium was M9 (19) supplemented with 0.2% sucrose or 0.2% glucose as the carbon source for *R. meliloti* or *Escherichia coli*, respectively. For growth of tryptophan auxotrophs, the minimal media was supplemented with tryptophan (20 μg/ml), indole (20 μg/ml), or anthranilate (20 μg/ml). Antibiotics were used at the following concentrations: neomycin, 200 μg/ml; spectinomycin, 100 μg/ml; streptomycin 400 μg/ml; and tetracycline, 10 μg/ml for *R. meliloti* and ampicillin, 50 μg/ml; neomycin, 50 μg/ml; spectinomycin, 100 μg/ml; and tetracycline, 15 μg/ml for *E. coli*.

Designation of the *R. meliloti trp* mutant genotype. *R. meliloti trp* mutants were assigned to genetic classes based

* Corresponding author.
† Present address: Genzyme Corp., Cambridge, MA 02142.
‡ Present address: Department of Biology, University of North Carolina at Chapel Hill, Chapel Hill, NC 27599.
§ Present address: Department of Biochemistry, University of Wisconsin, Madison, WI 53706.

TABLE 1. Bacterial strains and plasmids

Strain or plasmid	Relevant genotype or characteristic	Source or reference
R. meliloti strains		
Rm1021	SU47 Sm^r	F. Ausubel
Rm8614	Rm1021, *trpE(G)504*::Tn*5*	This work
Rm8694	Rm1021, *trpE(G)505*::Tn*5*	This work
Rm8695	Rm1021, *trpE(G)509*::Tn*5*	This work
Rm8699	Rm1021, *trpE(G)530*::Tn*5*	This work
Rm8691	Rm1021, *trpF519*::Tn*5*	This work
Rm8602	Rm1021, *trpC506*::Tn*5*	This work
Rm8612	Rm1021, *trpA521*::Tn*5*	This work
Rm8692	Rm1021, *trpB540*::Tn*5*	This work
Rm8736	Rm1021, *trpD541*::Tn*3*HoSp	This work
Rm8732	Rm1021, Δ*trpE(G)621*::Tn*5*	This work
Plasmids		
pRK600	pRK2013*npt*::Tn*9*	T. Finan (8a)
pBD26	pLAFR1 cosmid complementing *trpE(G)*	This work
pRml104	pLAFR1 cosmid complementing *trpC* and *trpD*	This work
pRml152	pLAFR1 cosmid complementing *trp*, *trpB*, and *trpF*	This work

upon growth response in M9 minimal medium supplemented with anthranilate, indole, or tryptophan and accumulation of tryptophan intermediates when the mutants were grown in minimal medium supplemented with growth-limiting concentrations of tryptophan (3 μg/ml) (25); the characteristics of other mutants within the same complementation group and complementation of defined *P. aeruginosa* PAO *trp* mutants have already been described (1, 15). *trpC* mutants were differentiated from *trpD* mutants on the basis of assay of phosphoribosyltransferase as described by Smith and Yanofsky (27).

Genetic manipulations, transposon mutagenesis, and Southern hybridization. pLAFR1 (9), pSUP202 (26), and their derivatives were mobilized by triparental matings by using helper plasmid pRK600 as described by Leigh et al. (16). Tn*5* mutants of strain Rm1021 were isolated in a manner similar to that of Beringer et al. (2). Mutants disrupted in the tryptophan biosynthetic pathway were originally identified as those which required addition of tryptophan for growth on minimal medium.

The Tn*5* insertions in *trpE(G)* mutants were mapped by Southern hybridization (data not shown) to independent sites within a 2.7-kb *Eco*RI fragment within the *R. meliloti* DNA carried by *trpE(G)* cosmid clone pBD26 (see Fig. 1).

Fusions to reporter genes were isolated by using transposons Tn*3*HoSp (11), Tn*3*Hog*us* (kindly supplied by Brian Staskowitz, University of California, Berkley), and Tn*3*-HoHoI by the method of Stachel et al. (29).

DNA manipulations and subcloning. Plasmid DNA was isolated from overnight cultures of *E. coli* by the alkaline lysis method (3). Chromosomal DNA was isolated by the method of Marmur (20). Restriction enzyme digests and ligations were performed in accordance with the specifications of the supplier (New England BioLabs, Beverly, Mass.). DNA probes were labelled by using a nick translation kit (Bethesda Research Laboratories, Gaithersburg, Md.), and Southern blotting (28) and hybridization on Gene Screen Plus (New England Nuclear, Boston, Mass.) were performed in accordance with the manufacturers' instructions.

Construction of a *trpE(G)* deletion. The Δ*trpE(G)621* deletion mutant was constructed in the following manner. First the 6.5-kb *trpE(G)*-containing *Bam*HI fragment (see Fig. 1) was cloned from pBD26 into suicide vector pSUP202 (26), which can be conjugated into *R. meliloti* but cannot replicate. Next, the 2.7-kb *Eco*RI fragment containing most of the *trpE(G)* coding region (see Fig. 1) was replaced with a cassette containing a spectinomycin resistance marker selectable in *R. meliloti* (8). The resultant disrupted *trpE(G)* gene was recombined into the Rm1021 chromosome by selecting for transconjugants which acquired spectinomycin resistance.

Nodulation assay. *R. meliloti* strains were screened for nodulation phenotypes on *M. sativa* cv. Iroquois seedlings as described by Leigh et al. (16). Each strain was tested on at least 10 plants. Seedlings were observed for nodule formation and growth over a 10-week period. For crushing, nodules were surface sterilized with 1% sodium hypochloride, washed with LB, and crushed in LB containing 2.5 mM $MgSO_4$, 2.5 mM $CaCl_2$, and 0.3 M glucose. Nitrogenase was assayed by using the acetylene reduction technique (30) on whole individual nodules.

Microscopy. Root nodules were excised from alfalfa roots 3 to 4 weeks after inoculation and fixed and prepared for microscopy as described by Hirsch et al. (13). Sections 0.5 μm thick were stained with multiple staining solution (Polysciences Inc., Warrington, Pa.) and examined under a light microscope.

Histological detection of β-glucuronidase activity. Nodules harvested 3 to 4 weeks after inoculation of plants were fixed on ice with 1% glutaradehyde and 0.1 M cacodylate, pH 7.2, for 2 h. After one freeze-thaw cycle, nodules were rinsed twice with Z buffer (0.05 M phosphate buffer, pH 7.0, containing 0.01 M KCl, 0.001 M $MgSO_4$, and 0.05 M β-mercaptoethanol) and stained in the same buffer containing 2 mM 5-bromo-4-chloro-3-indoyl-β-D-glucuronide (X-Glu; Sigma, St. Louis, Mo.). After being stained overnight at 37°C, nodules were affixed to a carrot slice with cyanoacrylate adhesive (Krazy Glue) and sectioned on a Polaron H1200 vibrating microtome (Bio-Rad Microscience Division, Cambridge, Mass.). Sections 50 μm thick were examined under a light microscope. Assays for β-glucuronidase activity were carried out by using the fluorometric substrate 4-methylumbelliferyl glucuronide (4-MU Glu). In preparation for the β-glucuronidase assay, bacteria from 1 ml of log-phase cells grown in LB medium were incubated in 0.1 ml of Z buffer containing 0.05% sodium cholate and 5 μl of toluene at 37°C for 10 min to permeablize their membranes. Assays for β-glucuronidase used 10 μl of permeablized cells in 100 μl of Z buffer containing 0.5 mg of 4-MU Glu at 37°C for 30 min. The reactions were quenched with 5 ml of 0.1 M glycine, pH 11, and the amount of 4-MU released was determined on a Turner 112 fluorometer set for excitation at 320 to 390 nm by reading the emission from the 4-MU product released at >415 nm. Micromoles of 4-MU released were determined by comparison to standard 4-MU solutions.

RESULTS

Isolation and characterization of Tn*5*-generated *trp* mutants of *R. meliloti*. By screening derivatives of *R. meliloti* Rm1021 that had been randomly mutagenized with transposon Tn*5*, we isolated 20 tryptophan auxotrophs. Recombinant plasmids that complemented these various tryptophan auxotrophs were then isolated from an *R. meliloti* library (9) by complementation. Consistent with the previous results of

TABLE 2. Characteristics of representative *R. meliloti trp* mutants

Tryptophan biosynthetic pathway step	*R. meliloti* mutation	Intermediate(s) accumulated	Growth on minimal media plus:			Complementing cosmid
			Anthranilate	Indole	Tryptophan	
Chorismate						
↓ TrpE(G)	*trpE(G)504*	ND[a]	+	+	+	pBD26
Anthranilate						
↓ TrpD	*trpD541*	Anthranilate	−	+	+	pRml104
Phosphoribosylanthranilate						
↓ TrpF	*trpF519*	Anthranilate	−	+	+	pRml152
1-(*o*-Carboxyphenylamino)-1-deoxyribulose-5-phosphate						
↓ TrpC	*trpC506*	Anthranilate	−	+	+	pRml104
Indoleglycerol phosphate						
↓ TrpAB	*trpA521*	Anthranilate, Indole	−	+	+	pRml152
Tryptophan	*trpB540*	Anthranilate, Indole	−	−	+	pRml152

[a] ND, not determined.

Johnston et al. (15), the tryptophan biosynthetic genes of *R. meliloti* were found to be grouped into three gene clusters. The individual *trp*::Tn*5* mutations were then assigned to various classes on the basis of complementation studies and growth response to and accumulation of Trp intermediates. The data from these experiments are summarized in Table 2.

Four of these mutants, represented in Table 2 by *trpE (G)505*, are of particular interest, since, as described below, they turned out to be the only class of *trp* mutants that exhibited symbiotic deficiencies. These mutants were assigned to the *trpE(G)* class on the basis of the following properties. They were able to grow on minimal media supplemented with anthranilate and did not accumulate anthranilate when grown with growth-limiting concentrations of tryptophan. This indicated they were blocked at the first step in tryptophan biosynthesis and were deficient in the *trpE(G)* gene product, anthranilate synthase. Each of these mutations was complemented by 40-kb plasmid pBD26, which was isolated from a broad-host-range cosmid bank of *R. meliloti* DNA (8). The Tn*5* insertions in each mapped to a 2.7-kb *Eco*RI fragment of the *R. meliloti* chromosome carried by pBD26. While this work was in progress, the DNA sequence that codes for the *R. meliloti* anthranilate synthase gene, including its promoter and putative leader peptide, was determined by Bae et al. (1). Southern hybridization experiments using a Tn*5* probe localized the positions of the Tn*5* insertions in the four *trpE(G)* mutants within the *trpE(G)* coding sequence (Fig. 1).

The Tn*5* insertions in five of the *trp* mutants fell into a second linkage group which contained the *R. meliloti trpD* and *trpC* genes. DNA sequencing and Southern hybridization experiments demonstrated that in two of these mutants,

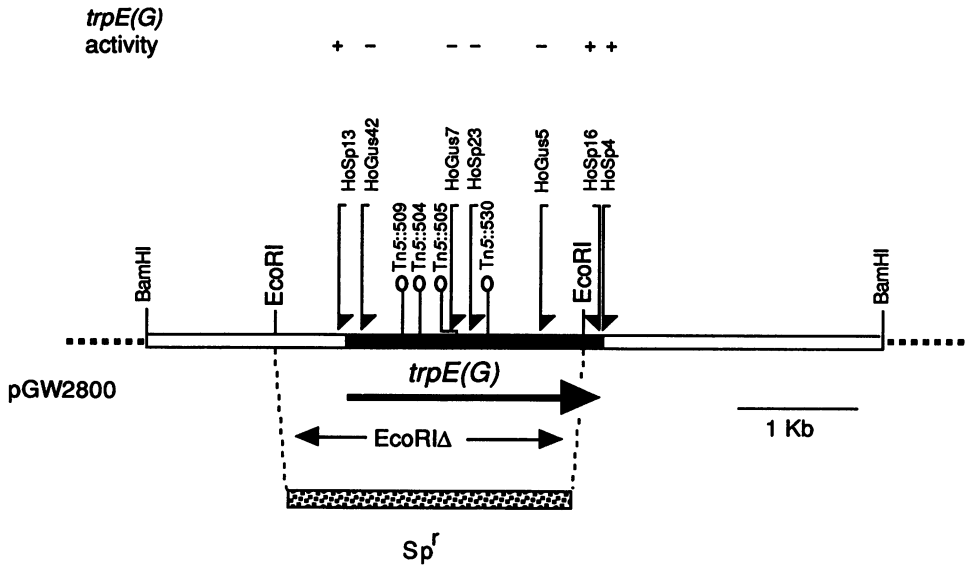

FIG. 1. Positions of transposon insertions in the *trpE(G)* region. The 6.5-kb *Bam*HI fragment containing the *R. meliloti trpE(G)* gene (open box) carried by pGW2800 is shown. The positions of transposon insertions within this fragment are indicated by arrows. The direction of transcription of the reporter gene within these insertions is toward the side which has the arrowhead. The *trpE(G)* coding sequence is indicated by the filled box (1). The *trpE(G)* complementing activity of plasmids carrying each insertion is indicated above each insertion. The relative positions of the Tn*5* insertions in each of the *R. meliloti trpE(G)* mutants are indicated by open circles.

represented in Table 2 by *trpC506*, Tn*5* was inserted within the *trpC* coding sequence (1a). The other three insertions were upstream of, and polar on, the *trpD* coding region. To examine the phenotype of a null *trpD* mutant, we therefore constructed *trpD502* by gene disruption by using transposon Tn*3*HoSp (11).

The remaining insertion mutants, represented by *trpA521*, *trpB1*, and *trpF519* in Table 2, were complemented by recombinant plasmid pRml152, which carried the third *trp* linkage group. The mutations in each were assigned to different loci on the basis of growth response to indole and whether or not indole was accumulated under tryptophan-limiting growth conditions.

***R. meliloti* mutants blocked in anthranilate synthesis are symbiotically defective.** When we screened the entire set of *R. meliloti trp* mutants for the symbiotic phenotype, we made the unexpected discovery that mutants blocked at the first step of this pathway, *trpE(G)*, were symbiotically defective but that mutants blocked at later steps in this biosynthetic pathway (Table 2), *trpA*, *trpB*, *trpC*, *trpD*, or *trpF*, were effective symbionts.

Plants inoculated with *R. meliloti trpE(G)*::Tn*5* mutants were stunted and chlorotic after 3 to 4 weeks of growth on nitrogen-free medium. This contrasted with the healthy green appearance of plants inoculated with *trpA*, *trpB*, *trpC*, *trpD*, or *trpF* mutants or with wild-type *R. meliloti*. The nodules that formed during the first 3 weeks were approximately the same size as those obtained with trp^+ rhizobia but were mostly white instead of pink. This suggested the possibility that (i) anthranilate biosynthesis, but not tryptophan biosynthesis, is required for successful nodulation of alfalfa by *R. meliloti*, (ii) the insertions in *trpE(G)* are polar on some downstream gene that is needed for effective symbiosis, or (iii) the *trpE(G)* gene product plays a role in nodulation unrelated to anthranilate biosynthesis.

Support for the first hypothesis, that anthranilate biosynthesis is required for effective symbiosis, was provided by our subsequent examination of the symbiotic properties of seven *R. meliloti aro*::Tn*5* mutants blocked in the aromatic amino acid biosynthetic pathway prior to chorismate synthesis (and therefore blocked before anthranilate biosynthesis). Plants inoculated with these *aro* mutants were stunted and chlorotic and carried Fix^- nodules that lacked nitrogenase activity at up to 3 weeks from inoculation. The nodules that formed on plants inoculated with the *aro* mutants resembled those elicited by *trpE(G)* mutants in that they were elongated and approximately the same size as the pink nodules induced by a wild-type strain but were white instead of pink.

After 3 to 4 weeks, some of the *trpE(G)*-inoculated plants began to fix nitrogen, as indicated by greening of the leaves and resumption of growth. Although most of the nodules on these Fix^+ plants were still white, a few markedly pink nodules were present. When these pink nodules were isolated, surface sterilized, and crushed, they were found to contain normal numbers of bacteria and bacteroids. However, the bacteria isolated from these pink effective nodules were neomycin sensitive and prototrophic, suggesting they had lost the Tn*5* insertion and regained *trpE(G)* function. There are three formal possibilities to account for this reversion: (i) precise excision of Tn*5*, (ii) imprecise excision that resulted in an altered but functional anthranilate synthase, and (iii) marker rescue of *trpE(G)*::Tn*5* by a cryptic *trpE(G)* analog or by a related gene, such as *pabA*.

Precise excision of Tn*5* appears to be the most likely hypothesis to account for the reversion of our *trpE(G)*::Tn*5* mutants. By 6 to 8 weeks postinoculation, most of the plants inoculated with any of the four *trpE(G)* Tn*5* mutants in our collection fixed nitrogen and had resumed growth. Since the Tn*5* insertions in these mutants were located at several sites across the *trpE(G)* coding region, the second possibility mentioned above appears unlikely. Marker rescue also seems unlikely, since seven *aro* mutants in our collection, which represent at least two complementation groups, have the same revertable phenotype as the *trpE(G)* mutants with respect to the appearance of a few Fix^+ nodules after 3 to 4 weeks. Therefore, the most likely mechanism for reversion of *trpE(G)*::Tn*5* appears to be precise excision of Tn*5*. Reversion of a *trpE(G)*::Tn*5* occurs at a frequency of less than 10^{-8} in the free-living state, suggesting that there is selection for revertants and that there may even be an increased frequency of precise excision of Tn*5* in planta.

Construction and characterization of a nonrevertable *trpE(G)* mutant. The instability of the *trpE(G)*::Tn*5* insertion mutants we had isolated made it difficult to assess the nature of the symbiotic deficiency caused by loss of *trpE(G)* function during prolonged nodulation experiments. To examine the symbiotic phenotype of *trpE(G)* mutants without the interference caused by excision of Tn*5*, we constructed a deletion, Δ*trpE(G)621*, by replacing the 2.7-kb *Eco*RI fragment (Fig. 1), which contains most of the *trpE(G)* coding sequence, with a spectinomycin resistance cassette. Details of the construction of this mutant are given in Materials and Methods, and the region deleted is shown in Fig. 1. Southern hybridization experiments using the 2.7-kb *Eco*RI fragment as a probe verified the deletion of *trpE(G)* in the Δ*trpE(G)621* mutant.

Plants inoculated with the Δ*trpE(G)621* mutant behaved in a manner similar to that of those inoculated with *trpE(G)*::Tn*5* mutants at up to 3 weeks from inoculation. After this period, many of the plants inoculated with the *trpE(G)*::Tn*5* mutants began to resume growth, apparently owing to precise excision of Tn*5* and restoration of *trpE(G)* function as described above. In contrast, plants inoculated with the Δ*trpE(G)* mutant continued to blanche and were dead by 7 to 8 weeks. Although 20 to 50% of these plants did not grow larger than uninoculated control plants (2 to 3 cm), the remainder did grow slightly (5 to 8 cm) but significantly less than plants inoculated with wild-type *R. meliloti* (15 cm).

Nodules induced by *trpE(G)* deletion mutants. The large nodules formed on alfalfa plants inoculated with the *trpE(G)* deletion mutant were of two morphological types, as determined by visual observation and direct assay of nitrogen-fixing ability by acetylene reduction. The first nodule type, A, was elongated and white but had a small pink zone at its base and was able to reduce acetylene. The second type, B, was also elongated and white but lacked the pink zone at its base and was unable to reduce acetylene. Type A nodules were observed at approximately one-third of the frequency of type B nodules. The finding that plants carrying type A nodules grew larger than the uninoculated controls suggests that these nodules were responsible for the limited nitrogen fixation that had occurred in these plants. In addition to the elongated nodules, we observed a number of small, round, white nodules, most of which lacked detectable nitrogen-fixing ability. We consider it likely that these were immature forms of type A and B nodules.

Examination of stained longitudinal cross sections of fixed type A and B nodules induced by the *trpE(G)* deletion mutant indicated that the Δ*trpE(G)621* mutation results in a block or delay at an intermediate stage in nodule development. Longitudinal cross sections from a normal nodule and

a type A nodule elicited by the Δ*trpE*(*G*) mutant are shown in Fig. 2. The normal nodule has five zones of cells as defined by Vasse et al. (31). The first zone distal to the plant root is made up of uninfected plant cells containing the nodule meristem. Zone II, or the infection zone, is made up of a few layers of cells just behind the nodule meristem and contains cells early in the infection process. Heavily vacuolated plant cells with visible nuclei containing few immature bacteroids are characteristic of this region. The first few layers of cells within the next zone have been defined as the zone II-zone III interzone and contain a profusion of starch granules or amyloplasts and are beginning to become packed with bacteroids. The nitrogen-fixing zone, III, makes up the bulk of the nodule. Cells within this zone are packed with bacteroids and have their intracellular organelles restricted close to the cell wall. Proximal to the plant root is zone IV, or the senescent zone. This zone contains the oldest infected cells within the nodule. Both bacteroid and cell membranes within this zone are beginning to degrade.

The structure of the Δ*trpE*(*G*)-induced type A nodule shown in Fig. 2B deviates significantly from that of a wild-type nodule. The cells contained in zones I and II are morphologically similar in both nodules, as illustrated by comparison under higher magnification in Fig. 3. The plant cells in this region are early in their symbiotic development and characteristically contain a discernible darkly staining nucleus, many large vacuoles, and a few immature bacteroids. In addition, infection threads indicated within this region of nodules induced by both wild-type and *trpE*(*G*) rhizobia appear similar. These observations suggest that the early stages in symbiotic development induced by *trpE*(*G*) mutants proceed normally.

In contrast to the normal nodule, in which cells characteristic of the infection zone are found localized to a small region (zone II) just behind the nodule meristem, in a Δ*trpE*(*G*)-induced type A nodule they are found over a much more extensive region encompassing approximately two-thirds of the nodule. The cells in this extended early symbiotic zone of type A nodules largely resemble those found in zone II of normal nodules, except that there appear to be more starch granules (amyloplasts), a characteristic of cells normally found in the zone II-zone III interzone of normal or ineffective nodules (31). The rest of a type A nodule (proximal to the plant) consists of cells packed with differentiated bacteroids and resembles zone III of nodules elicited by wild-type rhizobia. However, unlike a normal nodule, in which this zone occupies most of the nodule, it encompasses only the proximal quarter of the Δ*trpE*(*G*)-induced nodule. This corresponds to the region of the nodules that was pink and presumably is where nitrogen fixation occurs.

Type B nodules elicited by Δ*trpE*(*G*) mutants contained no cells packed with bacteroids, consistent with the fact that nitrogen fixation was not detected. A representative cross section of a type B nodule is shown in Fig. 4. As with the type A nodules, the meristematic region and the early infection zone appeared similar to those of wild-type nodules. The extent of the zone II-like region varied from nodule to nodule, but in general the region was more extended than in nodules elicited by wild-type rhizobia but less extended than in type A nodules. The example illustrated in Fig. 4 was typical, with the zone II-like region extending approximately halfway down the nodule. Immediately after the zone II-like region of type B nodules, there was a band of cells containing a profusion of amyloplasts and infected cells. The remaining region of the type B nodules, proximal to the root, usually represented one-third or more of the nodule and consisted of empty cells that lacked detectable bacteria, bacteroids, infection threads, nuclei, or amyloplasts (Fig. 5).

All of the *trpE*(*G*)-induced nodule types contained bacteria, but only the Fix$^+$, elongated nodules contained significant numbers of bacteroids. When crushed, both type A and type B nodules were found to contain about 10^3 rhizobia, comparable to numbers recovered from nodules induced by the wild type. The rhizobia recovered from these nodules were all spectinomycin resistant and Trp$^-$, suggesting that they still carried the original *trpE*(*G*) deletion. When the Trp$^-$ bacteria isolated from these crushed nodules were used to inoculate plants, their symbiotic phenotypes were indistinguishable from those of the original *trpE*(*G*) deletion mutant.

The symbiotic defect in *trpE*(*G*) mutants is due to disruption of the *trpE*(*G*) gene. Since all of the available *trpE*(*G*) mutants were generated by insertion of DNA, we were concerned that the symbiotic deficiency of these mutants might not be due to loss of *trpE*(*G*) function but rather to a polar effect of these insertions on some previously unknown symbiotic gene located downstream of *trpE*(*G*). To address this issue directly, we constructed a strain containing a Tn*3*HoSp insertion downstream of the *trpE*(*G*) coding sequence and analyzed its symbiotic phenotype. The map shown in Fig. 1 illustrates the locations of insertions in the *trpE*(*G*) region and the results of *trpE*(*G*) complementation with plasmids containing these insertions. Strains containing insertion Tn*3*HoSp23, which is within the *trpE*(*G*) coding sequence, or Tn*3*HoSp4, located just downstream of the *trpE*(*G*) coding sequence, were constructed by marker exchange. The strain carrying the Tn*3*HoSp23 insertion had the Fix$^-$ symbiotic phenotype described above for *trpE*(*G*)::Tn*5* mutants. In contrast, the strain carrying the Tn*3*HoSp4 insertion was Fix$^+$. Since the *trpE*(*G*) terminator (1) and the Tn*3*HoSp4 insert are within 40 bp of the anthranilate synthase stop codon, we concluded that the symbiotic defect in *trpE*(*G*) insertion mutants is unlikely to be due to polar effects on a downstream gene.

Histological localization of *trpE*(*G*) expression in nodules. To examine the expression of *trpE*(*G*) in planta, we used transposon Tn*3*Ho*gus* to construct *trpE*(*G*)-*gus* gene fusions which expressed β-glucuronidase as a reporter of *trpE*(*G*) gene expression. β-Glucuronidase activity is a useful histological reporter in *R. meliloti*-alfalfa symbiosis, since neither the bacterium nor alfalfa produces a detectable background of β-glucuronidase activity (25), thus allowing histological localization of gene expression within the nodule by using the β-glucuronidase-specific stain X-Glu. We isolated three derivatives of pBD26 which carried Tn*3*Ho*gus* insertions which inactivated *trpE*(*G*) complementing activity and expressed β-glucuronidase activity ex planta, as indicated by their blueness when they were grown on medium containing the β-glucuronidase chromogenic substrate X-Glu. The relative positions of these insertions are shown in Fig. 1.

To examine expression of a *trp* gene required later in the tryptophan biosynthetic pathway but not for symbiotic function, we also isolated a derivative of pRml152 carrying a Tn*3*Ho*gus* insertion in the *trpABF* gene cluster which inactivated *trpA* complementing activity and expressed β-glucuronidase activity ex planta.

Alfalfa seedlings were inoculated with derivatives of parental strain Rm1021 that carried either a plasmid-borne *trpE*(*G*)-*gus* fusion or a *trpA*-*gus* fusion, and the resulting nodules were sectioned and stained for β-glucuronidase activity. As shown in Fig. 6, the regions of the nodule that contain bacteroids stained strongly with X-Glu, indicating

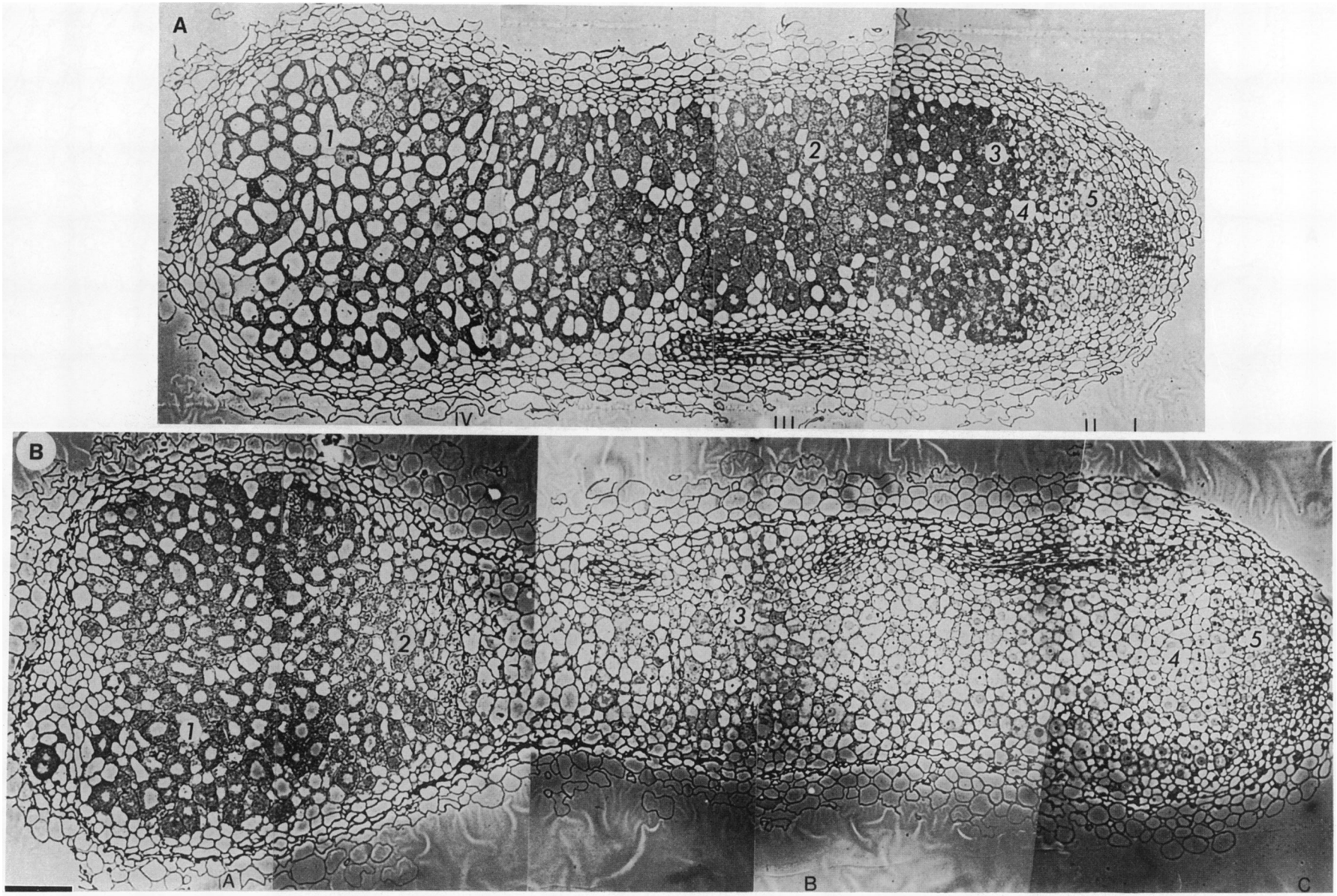

FIG. 2. Histology of alfalfa nodules induced by wild-type and *trpE(G)* mutant *R. meliloti*. Longitudinal sections of 4-week-old alfalfa nodules induced by Rm1021 (A) and a type A nodule induced by Rm8732 [Δ*trpE(G)621*] (B) are shown. The meristematic, infection, nitrogen-fixing, and senescent zones of the Rm1021-induced nodule are labelled zones I to IV, respectively. Corresponding symbiotic, infectionlike, and meristematic zones of the Rm8732-induced nodule are labeled A to C, respectively. Numbers 1 to 5 indicate regions shown at higher magnification in Fig. 4. Bar, 100 μm.

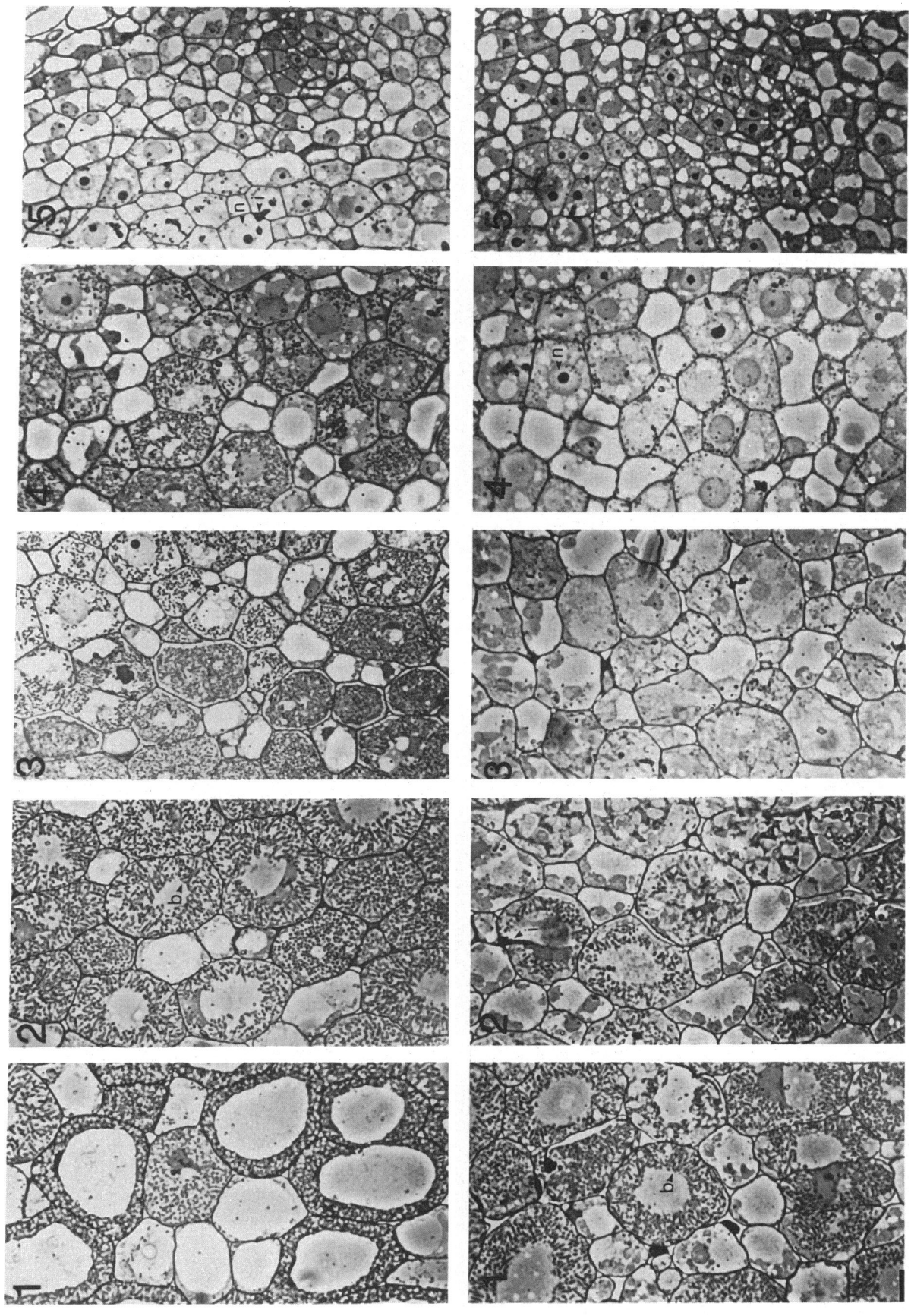

FIG. 3. Histological comparison regions of an alfalfa nodule induced by Rm1021 (A) and a type A nodule induced by Rm8732 [*ΔtrpE(G)621*] (B). Regions shown from sections of an Rm1021-induced nodule are zone I (A, panel 5), the zone II-zone III interzone (A, panels 3 and 4), zone III (A, panel 2), and zone IV (A, panel 1). Regions of the Rm8732-induced nodule are the meristematic and early infection zones (B, panel 5), the infectionlike zone (B, panels 3 and 4), the zone like the zone II-zone III interzone (B, panel 2), and the nitrogen-fixing zone (B, panel 1) from a type A nodule. Bacteroids (b), infection threads (i), amyloplasts (a), and nuclei (n) are indicated. The number at the upper left of each region corresponds to the relative position of the corresponding number in Fig. 2. Bar, 10 μm.

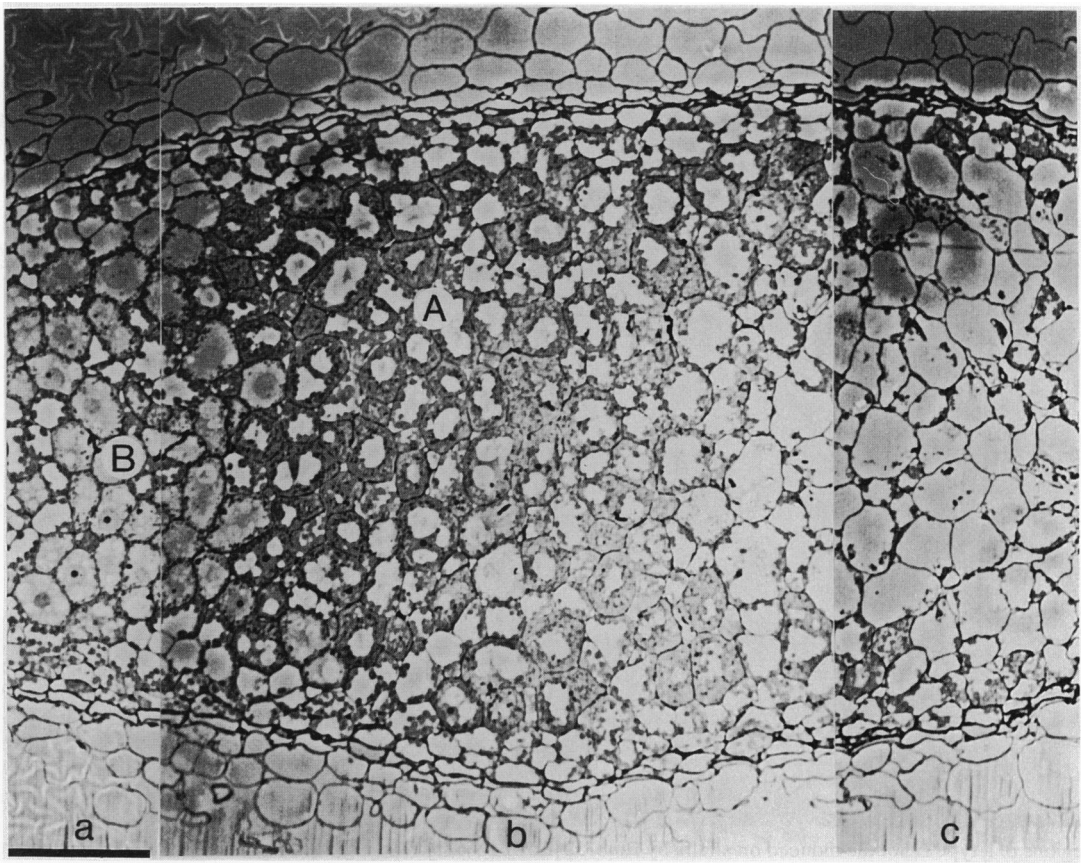

FIG. 4. Histology of type B nodule induced by Rm8732 [Δ*trpE*(*G*)*621*] on *M. sativa*. The infectionlike zone (a), the zone like the zone II-zone III interzone (b), and the senescent zone (c) are shown. The regions designated A and B are shown at a higher magnification in Fig. 6. Bar, 100 μm.

that *trpE*(*G*) is expressed in the bacteroid state. We were not able to detect β-glucuronidase activity in the nodule elicited by the derivative carrying the *trpA-gus* fusion (Fig. 6). However, since the level of expression of the *trpA-gus* fusion was 12-fold lower than that of the *trpE*(*G*)-*gus* fusion in the free-living state (data not shown), it was possible that our failure to detect *trpA* expression was due to insufficient sensitivity in the cytological staining. Our failure to detect *trpA* expression was, however, consistent with the failure to detect *trpA* mRNA in nodules (18).

DISCUSSION

The *trpE*(*G*) gene of *R. meliloti* encodes anthranilate synthase, the first enzyme in the tryptophan biosynthetic pathway. We have shown that insertion and deletion *trpE*(*G*) mutants of *R. meliloti* form two classes of unusual elongated nodules on alfalfa that are distinguished by their extended invasion zones. Type A nodules, which have pink bases and are capable of limited nitrogen fixation, contain cells packed with bacteroids at their bases. Type B nodules, which do not have pink bases and do not fix nitrogen, do not contain bacteroids. Genetic experiments have strongly suggested that the symbiotic deficiencies of these *trpE*(*G*) mutants are not due to polar effects of the *trpE*(*G*) mutations on some downstream gene but rather are due to the loss of *trpE*(*G*) function itself. Furthermore, we found that *R. meliloti* derivatives carrying mutations in genes necessary for later steps in the tryptophan biosynthetic pathway, *trpD*, *trpF*, *trpC*, *trpA*, and *trpB*, formed Fix$^+$ nodules. These findings indicate that *R. meliloti* requires *trpE*(*G*) function to carry out normal nodulation of alfalfa but does not require the function of the other tryptophan biosynthetic genes.

The simplest interpretation of these results is that normal nodulation of alfalfa by *R. meliloti* requires bacterial synthesis of anthranilate but not bacterial synthesis of tryptophan. This interpretation is supported by the finding that *R. meliloti aro* mutants, which are blocked prior to anthranilate synthesis, exhibit symbiotic deficiencies similar to those of *trpE*(*G*) mutants. Furthermore, our finding of *trpE*(*G*) expression in nodules, coupled with our failure to detect *trpAB* expression, is consistent with this interpretation. We have not ruled out the formal possibility that the *R. meliloti trpE*(*G*) gene product has a second symbiotic function that is unrelated to anthranilate biosynthesis. However, the very strong homology of the deduced amino acid sequence of the *R. meliloti trpE*(*G*) gene product to other anthranilate synthases (1), when taken together with the observed symbiotic deficiencies of *R. meliloti aro* mutants, makes this class of explanation seem unlikely.

The symbiotic deficiencies caused by *trpE*(*G*) mutations appear to be different from those caused by mutations in previously described symbiotic genes of *R. meliloti*. Not only do nodules elicited by *trpE*(*G*) mutants have a novel structure, but the nature of the block in nodule development in type A nodules varies within the nodule as a function of

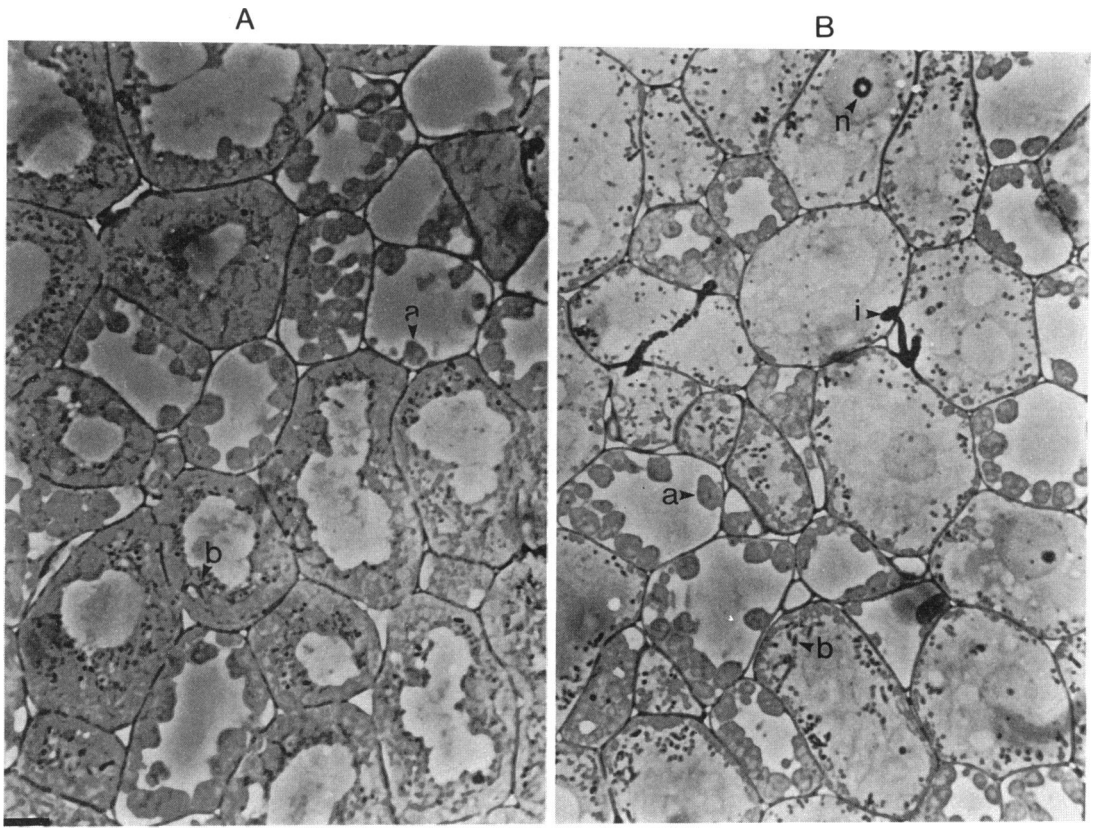

FIG. 5. Regions of a type B nodule induced on alfalfa by Rm8732 [Δ*trpE*(*G*)*621*]. The regions shown are from the zone like the zone II-zone III interzone and from the infectionlike zone. Infection threads (i), immature bacteroids (b), amyloplasts (a), and nuclei (n) are indicated. Bar, 10 μm.

the distance from the root. Mutations in previously described symbiotic genes appear to block nodulation at some characteristic stage. For example, *nod* mutants fail to elicit nodules, *ndv* and *exo* mutants elicit nodules but fail to invade them, *leu* and *hemA* mutations block nodulation just before release of the rhizobia from the infection thread, *dctA* mutations block bacteroid development, and *nif* and *fix* mutations block the process at a very late stage (5, 7). The type A nodules elicited by *trpE*(*G*) mutants are unusual in that they contain cells packed with nitrogen-fixing bacteroids near the base of the nodules, suggesting that in that region of the nodule, the bacteria are able to differentiate into mature nitrogen-fixing bacteroids. Yet farther from the base, much of the nodule resembles zone II of wild-type nodules. This suggests that in that more distal region of the nodule, the rhizobia are not able to differentiate into nitrogen-fixing bacteroids. Since nodules grow from their tips, there is a direct relationship between the physical position of plant cells within the nodule and the chronological appearance of those plant cells. Thus, it is possible to describe the symbiotic deficiencies of type A nodules equivalently by saying that the *trpE*(*G*) mutants are able to differentiate successfully into bacteroids up to some time after nodule initiation but are not able to differentiate into nitrogen-fixing bacteroids after that time. We feel that the transition from a zone II-like region to nitrogen-fixing bacteroid-containing cells observed in type A nodules is more likely to be a consequence of distance from the root rather than a consequence of the time after nodule initiation, since nodules with the type A characteristics kept appearing and developing over a period of several weeks after the initial inoculation. Thus, we hypothesize that in nodulation of alfalfa by *R. meliloti trpE*(*G*) mutants, symbiotic development is limited by the absence of

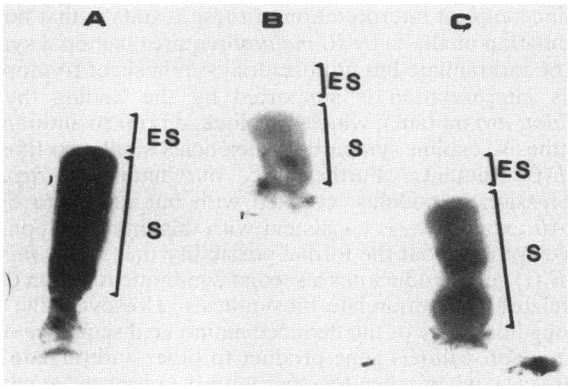

FIG. 6. Histological staining for expression of *R. meliloti trp* genes. Thick sections of nodules induced by *R. meliloti* carrying pBD26*trpE*::Tn*3*HoGus7 (A), *R. meliloti* carrying pRml152 *trpA*::Tn*3*HoGus (B), and wild-type *R. meliloti* (C) stained for β-glucuronidase activity with X-Glu. Symbiotic (S) and early symbiotic (ES) regions of each are indicated. Only the nodule induced by *R. meliloti* carrying the *trpE*(*G*)::*gus* fusion stained blue in this histological assay, as indicated by its darkness in this black-and-white photograph.

some factor and this limitation can be overcome in plant cells that are proximal to the root but not in plant cells that are more distal from the root. It is also possible that the limitation of such a factor is responsible for the failure of the bacteroids in type A nodules to exhibit the senescence that is observed in the corresponding position in wild-type nodules.

In such a model, the limiting factor could be anthranilate itself or some factor derived from anthranilate. With respect to the first possibility, an attractive model we are considering is that anthranilate functions as an in planta siderophore and that the symbiotic block observed in cells more distal from the base of the nodule is a consequence of failure of the bacteria to import sufficient iron to allow development into nitrogen-fixing bacteroids. Anthranilate has previously been shown to function as a siderophore for *R. leguminosarum* (23, 24). There is an increased demand for iron during bacteroid development because of the need to synthesize heme and the various iron-containing proteins necessary for nitrogen fixation, which contain 30 to 40 atoms of an iron-enzyme complex (32). For example, nitrogenase can constitute 10 to 12% of the total protein in a bacterial cell and the bacteria also synthesize the heme moeity of leghemoglobin, which can represent as much as 25 to 30% of the total soluble protein in infected plant cells (12). *R. meliloti* Rm1021 possesses a high-affinity iron transport system that utilizes a novel siderophore with an unknown structure (10). However, it is possible that utilization of such a high-affinity iron transport system in planta is incompatible with development of a symbiotic relationship with the plant. The fact that *R. meliloti* mutants lacking this high-affinity transport system have only very slight symbiotic deficiencies (10) is consistent with the hypothesis that the bacteria use a different iron transport system in planta. With respect to the second possibility, that the putative limiting factor is a compound derived from anthranilate, it is interesting that anthranilate represents the first step towards the synthesis of an indole ring and that plant hormones such as indole-3-acetic acid contain an indole ring.

Both the type A and type B nodules differ from those induced by *ndv*, *exoD*, and other *exo* mutants in that they become very elongated. In the case of the type B nodules, this elongation occurs without the obvious appearance of mature bacteroids typical of zone III, suggesting that release of the bacteria from the infection thread is important for nodule elongation but differentiation into bacteroids is not. We have no good explanation for the appearance of the type B nodules, as well as the type A nodules, since both classes of nodules continued to appear over an extended time and within the same general regions on the roots. There appears to be some type of microheterogeneity within the root tissue that is responsible for this.

It is possible that nodules elicited by *trpE(G)* mutants will ultimately prove to be useful in biochemical characterizations of cells within the invasion zone. Normally, cells in the part of the nodule classified as zone II constitute a very small fraction of a wild-type nodule. In contrast, in nodules elicited by *R. meliloti trpE(G)* mutants a zone II-like region can constitute as much as two-thirds of the nodule.

ACKNOWLEDGMENTS

The *trp* mutants were isolated in 7.031, an undergraduate project laboratory taught by G.C.W. and taken by K.L. The symbiotic deficiency of the *trpE(G)* mutants was noted by G.C.W. while on sabbatical in Sharon Long's laboratory and we thank her for her comments and interest.

K.L. was subsequently supported by the Undergraduate Research Opportunities Program at the Massachusetts Institute of Technology. The preliminary phase of this work was supported by a grant from W.R. Grace, and the subsequent work was supported by Public Health Service grant GM31030.

REFERENCES

1. **Bae, Y. M., E. Holmgren, and I. P. Crawford.** 1989. *Rhizobium meliloti* anthranilate synthase gene: cloning, sequence, and expression in *Escherichia coli*. J. Bacteriol. **171**:3471–3478.
1a. **Barsomian, G. D., and G. C. Walker.** Unpublished data.
2. **Beringer, J. E., J. L. Benyon, A. V. Buchanan-Wollaston, and A. W. B. Johnston.** 1978. Transfer of the drug-resistance transposon Tn*5* to *Rhizobium*. Nature (London) **276**:633–634.
3. **Birnboim, H. C., and J. Doly.** 1979. A rapid alkaline extraction procedure for screening recombinant plasmid DNA. Nucleic Acids Res. **7**:1513–1523.
4. **Crawford, I. P.** 1989. Evolution of a biosynthetic pathway: the tryptophan paradigm. Annu. Rev. Microbiol. **43**:567–600.
5. **Dickstein, R., and F. M. Ausubel (Harvard University).** 1990. Personal communication.
6. **Downie, J. A., and A. W. B. Johnston.** 1986. Nodulation of legumes by Rhizobium: the recognized root? Cell **47**:153–154.
7. **Earl, C. D., C. Ronson, and F. M. Ausubel.** 1987. Genetic and structural analysis of the *Rhizobium meliloti fixA*, *fixB*, *fixC*, and *fixX* genes. J. Bacteriol. **169**:1127–1136.
8. **Fellay, R., J. Frey, and H. Krisch.** 1987. Interposon mutagenesis of soil and water bacteria: a family of DNA fragments designed for in vitro insertional mutagenesis of Gram-negative bacteria. Gene **52**:147–154.
8a. **Finan, T. M., B. Kunkel, G. F. De Vos, and E. R. Signer.** 1986. Second symbiotic megaplasmid in *Rhizobium meliloti* carrying exopolysaccharide and thiamine synthesis genes. J. Bacteriol. **167**:66–72.
9. **Friedman, A. M., S. R. Long, S. E. Brown, W. J. Buikema, and F. M. Ausubel.** 1982. Construction of a broad host range cosmid cloning vector and its use in genetic analysis of Rhizobium mutants. Gene **18**:289–296.
10. **Gill, P. R., L. L. Barton, M. D. Scoble, and J. B. Neilands.** 1991. A high-affinity iron transport system of Rhizobium meliloti may be required for efficient nitrogen-fixation *in planta*. Plant Soil **130**:211–217.
11. **Glazebrook, J., and G. C. Walker.** 1989. A novel exopolysaccharide can function in place of the calcofluor-binding exopolysaccharide in nodulation of alfalfa by *Rhizobium meliloti*. Cell **56**:661–672.
12. **Guerinot, M. L.** 1991. Iron uptake and metabolism in the rhizobium/legume symbiosis. Plant Soil **130**:190–209.
13. **Hirsch, A. M., M. Bang, and F. M. Ausubel.** 1983. Ultrastructure analysis of ineffective nodules formed by *nif*::Tn*5* mutants of *Rhizobium meliloti*. J. Bacteriol. **155**:367–380.
14. **Hodgson, A. L. M., and G. Stacey.** 1986. Potential for *Rhizobium* improvement. Crit. Rev. Biotechnol. **4**:1–74.
15. **Johnston, A. W. B., M. J. Bibb, and J. E. Beringer.** 1978. Tryptophan genes in *Rhizobium*—their organization and their transfer to other bacterial genera. Mol. Gen. Genet. **165**:323–3●●.
16. **Leigh, J. A., E. R. Signer, and G. C. Walker.** 1985. Exopolysaccharide-deficient mutants of *Rhizobium meliloti* that form ineffective nodules. Proc. Natl. Acad. Sci. USA **82**:6231–6235.
17. **Long, S. R.** 1989. *Rhizobium* genetics. Annu. Rev. Genet. **23**:483–506.
18. **Long, S. R. (Stanford University).** 1991. Personal communication.
19. **Maniatis, T., E. F. Fritsch, and J. Sambrook.** 1982. Molecular cloning: a laboratory manual. Cold Spring Harbor Laboratory, Cold Spring Harbor, N.Y.
20. **Marmur, J.** 1961. A procedure for the isolation of deoxyribonucleic acid from micro-organisms. J. Mol. Biol. **3**:208–218.
21. **Nap, J., and T. Bisseling.** 1990. Developmental biology of a plant-prokaryote symbiosis: the legume root nodule. Science **250**:948–954.
22. **Newcomb, W.** 1981. Nodule morphogenesis and differentiation.

Int. Rev. Cytol. **13**(Suppl.):247–298.
23. **Rioux, C. R., D. C. Jordan, and J. B. M. Rattray.** 1986. Iron requirement of *Rhizobium leguminosarum* and secretion of anthranilic acid during growth on an iron-deficient medium. Arch. Biochem. Biophys. **248:**175–182.
24. **Rioux, C. R., D. C. Jordan, and J. B. M. Rattray.** 1986. Anthranilate-promoted iron uptake in *Rhizobium leguminosarum*. Arch. Biochem. Biophys. **248:**183–189.
25. **Sharma, S. B., and E. R. Signer.** 1990. Temporal and spatial regulation of the symbiotic genes of *Rhizobium meliloti in planta* revealed by transposon Tn*5-gusA*. Genes Dev. **4:**344–356.
26. **Simon, R., M. O'Connell, M. Labes, and A. Puhler.** 1986. Plasmid vectors for the genetic analysis and manipulation of rhizobia and other gram-negative bacteria. Methods Enzymol. **118:**640–659.
27. **Smith, O. H., and C. Yanofsky.** 1962. Enzymes involved in the biosynthesis of tryptophan. Methods Enzymol. **V:**794–807.
28. **Southern, E. M.** 1979. Gel electrophoresis of restriction fragments. Methods Enzymol. **68:**152–176.
29. **Stachel, S. E., G. An, C. Flores, and E. W. Nester.** 1985. A Tn*3* *lacZ* transposon for the random generation of β-galactosidase gene fusions: application to the analysis of gene expression in *Agrobacterium*. EMBO **4:**891–898.
30. **Turner, G. L., and A. H. Gibson.** 1980. Measurement of nitrogen fixation by indirect means, p. 111–138. *In* F. J. Bergersen (ed.), Methods for evaluating biological nitrogen fixation. Wiley, Chichester, England.
31. **Vasse, J., F. De Billy, S. Camut, and G. Truchet.** 1990. Correlation between ultrastructural differentiation of bacteroids and nitrogen fixation in alfalfa nodules. J. Bacteriol. **172:**4295–4306.
32. **Walsh, C.** 1979. Enzymatic reaction mechanisms, p. 439. W. H. Freeman & Co., San Francisco.